CAM-CLAY and Hydraulic Conductivity Diagram Relations in Consolidated and Sheared Clay-Matrices

D. Gélard[1], P Dudoignon[2], A. Pantet[2] and S. Sammartino[2]

[1]*L.T.H.E. UMR 5564 (CNRS, INPG, IRD, UJF), 1209 rue de la piscine, Dom. Univ. De St Martin d'Hères, BP 53, 38041 Grenoble cedex 9, FRANCE*

[2]*Ecole Supérieure d'Ingénieurs de Poitiers, UMR CNRS 6532 "HydrASA", Etude Recherche Matériaux, 40, avenue du Recteur Pineau,86022 Poitiers cedex FRANCE*

email : patrick.dudoignon@esip.univ-poitiers.fr

1. SUMMARY

Methods of image analyses, carried out on thin sections made in consolidated and sheared kaolinite test pieces, allow the identification of three "microstructural domains": (1) the initial isotropic matrix, (2) the partly anisotropic matrix due to simple particle arrangement, and (3) the anisotropic matrix due to arrangement plus crushing and stretching of particles, in the shear plane domain. In order to explain the micromechanisms of the clay matrix behaviour, this paper proposes to link the "microstructural domains" represented in the e versus log p CAM-CLAY diagram and domains of hydraulic conductivity in the k versus e diagram. The hydraulic conductivities are calculated following the Kozeny-Carman relations, which take into account the micro-arrangement of particles, via a tortuosity calculated from image analyses at the microscopic scale on the clay-material. The generation of 2D images shows that the particle rearrangement is in part governed by the lower limits of porosity in the material from its isotropic to its anisotropic state. The microtexture behaviour, induced by the superimposition of the compaction, orientation and particle stretching stages, causes an anisotropy of k which acts (1) on the interstitial water flow direction, (2) on the rotation of particles itself, and (3) on the damage mechanism of the clay.

2. INTRODUCTION

The relations between macroscopic properties of a clayey material and its microtexture evolution when it is submitted to mechanical stresses, are complex and not clearly formalised. However, the arrangement of particles and pores is a major factor in the rheological and hydraulic properties of the material from the flocculation mechanisms to the soil compaction /1, 2, 3, 4, 5, 6, 7/. Due to the micrometric size of clay

mineral crystals, qualitative descriptions of microtexture were currently made by Scanning Electron Microscope (SEM) and Transmission Electron Microscope (TEM) investigations /8, 9, 10, 11/. But several scientists have demonstrated that optical microscopy, using the birefringence properties of crystallites, is well suited to this quantitative investigation /12, 13, 14/.

The present work is based on the microscopy image analysis of thin sections made in kaolinite test pieces after consolidation and shearing in a triaxial apparatus /14/. In order to explain the elementary mechanisms of material deformation, displacement or damage of clay fabric during mechanical stress, this paper proposes to link:

- firstly the particle arrangement in the clay matrix during the successive steps of consolidation and shearing with the intrinsic hydraulic conductivity changes,
- and secondly the state trend of the sample in the e versus log p CAM-CLAY representation with an hydraulic conductivity trend in the k versus e diagram.

Material, Method, and CAM-CLAY representation

The studied material consists of cylindrical kaolinite test pieces that have been sheared with a triaxial test apparatus. The test pieces (35 mm diameter and 70 mm high) have been cut in mushy paste of kaolinite and distilled water mixture. The initial water content of the paste is 50% in weight. The dried volumic mass is 11.7 kN/m^3 and the void ratio is 1.25 /14/. The specific surface of the kaolinite measured by methylen blue absorption is 34.4 m^2/g. The laser granulometry gives a large distribution of the particle size with 45% of the particles ranging from 3 to 15 μm. The average specific surface calculated from the different granulometries is 52.1 m^2/g.

Chronologically two experiment series were performed on saturated samples with the (consolidated and drained) triaxial test apparatus /13, 14/:

(1) the isotropic and hydrostatic consolidation tests

(2) the shearing tests on normal consolidated samples and on over-consolidated samples.

The shear tests were conducted up to significant post peak deformation. The triaxial cell is a WF 10201 Wykeham Farrance equipped with a Tritech 50 loading device.

3. RESULTS

The shear tests performed on normal consolidated samples at 100, 300, 400, and 600 kPa define the Critical State Line (CSL) projection parallel to the Virgin Consolidation Line (VCL) projection (λ'=-0.34) with a void ratio variation e_0-e_c = 0.10 (Fig. 2(a)). Two series of shear tests were performed on over-consolidated samples (σ_{cons} = 600kPa, σ_{sh} = 300, 200, 100 kPa and σ_{cons} = 300kPa, σ_{sh} = 200, 100 kPa). The increasing of the σ_{cons} - σ_{sh} induces the decrease of the e_0-e_c values from 0.10 for normal consolidated

samples to 0.03, 0.02, and 0.01 values for over-consolidated samples respectively.

The observations on thin sections, coupling the optical microscope and an image analysis system, are based on the kaolinite birefringence properties ratio, and measurements of the porosity at the microsite scale were performed by S.E.M. chemical microanalyses [13, 14]. The anisotropy percentage is calculated from the mathematical decomposition of the grey level diagrams characteristic of the analysed microsites. The grey level curves are decomposed in gaussian components. The anisotropy percentage is defined as the ratio:

Anisotropy % = anisotropic gaussian component area /
(anisotropic gaussian component area + isotropic gaussian component area)

Finally, the rearrangement of the particles in the kaolinitic material may be sketched in the e versus log p CAM-CLAY diagram by the following domains (Fig. 2(a)):

(1) the isotropic domain located between the VCL and CSL projections. Its base is the $I_{600} - I_{100}$ over-consolidation line. It includes the isotropic consolidation trends. The simple decreasing of the initial consolidation pressure induces a minor increasing of the void ratio and suggests a conservation of the isotropic texture (I_{600} to I_{100} trend).

(2) the shearing domain located between the $I_{600} - I_{100}$ over-consolidation line and CSL projection. It induces an anisotropy of the microtexture by a progressive rearrangement of the particles towards a face to face organisation.

(3) the domain located between the CSL projection and the "shear plane line". The anisotropy % increases up to 100% on the "shear band line". The face-to-face arrangement of the particles is progressively associated to the particle stretching.

Microtexture and hydraulic conductivity

The hydraulic conductivity calculations and modelling have to include the heterogeneity of the particle arrangements, the associated void ratio and the specific surface of the material. The equations of Kozeny-Carman take into account all these micrometric parameters via a tortuosity (T) calculation /15, 16/:

$$Kk = [1/(2\ T^2)][n^3/(Ssp)^2]$$

$Ssp = S\ (1-n)$ with S = surface area = particle area/particle volume.

The tortuosity of fluid pathways is not directly measurable. However, the tortuosity still remains a well-known and useful fitting parameter /17, 18/. In this work, we tried to find solutions to calculate it, taking into account the spatial arrangement of particles in this fine divided kind of media. Two contributions may be distinguished in this investigation: (1) the 2D simplified modelling of the media based on petrographic observations and quantification (particle arrangement) (2) the tortuosity calculation with the help of image analysis tools and Monte Carlo simulation /19, 20/.

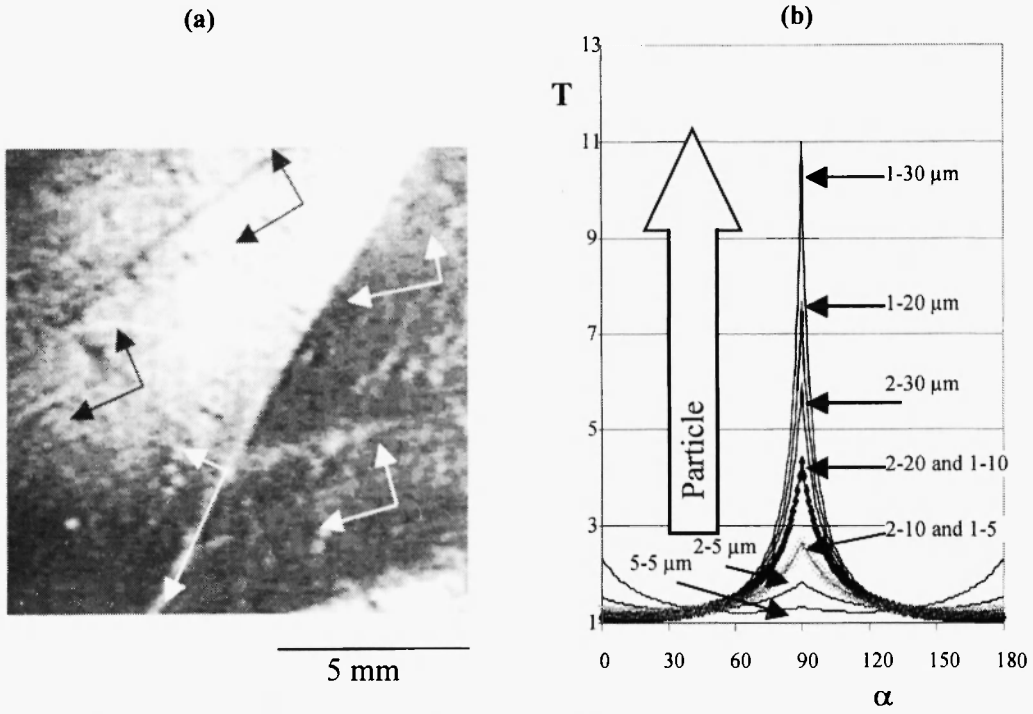

Fig. 1: (a) Photograph of oriented and sheared clay matrix (optical microscope - polarized light; arrows indicate the calculated k anisotropy). (b) The tortuosity drastically increases with the lengthening of particles. T = tortuosity, a = orientation of particles in comparison with direct path way of fluid.

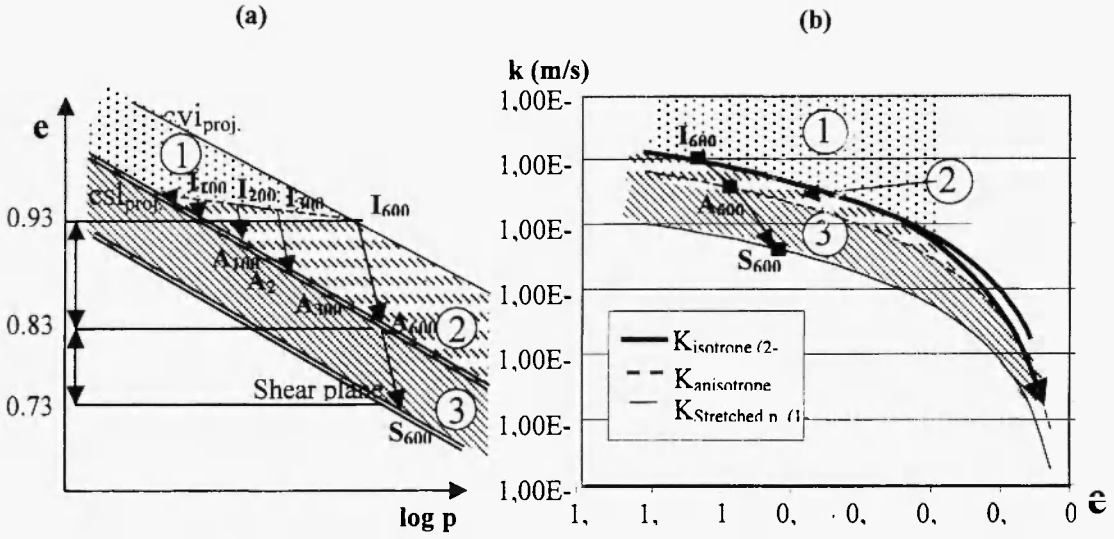

Fig. 2: (a) - CAM-CLAY diagram and (b) - hydraulic conductivity curve relations for the consolidated (600 kPa) and sheared kaolinitic matrix. e = void ratio, p = average pressure, k = hydraulic conductivity.

1) Analytical approach

For each microsite of the material complementary mechanical and petrographic investigations give the value of porosity, anisotropy %, and the mean orientation of particles. In such conditions, tortuosity may be calculated considering three media: (1) porosity, (2) the isotropic part of the media (faces of isotropically distributed particles) and (3) the anisotropic part of the media (faces of the parallel particles). The tortuosity is defined as:

$$T = (Lp + Li + La) / L$$

where Lp is the equivalent length in the porosity, Li and La are the cumulated length (D/2) and width (d) of the N crystallites followed by the fluid way, in isotropic and anisotropic medium respectively. The number of steps (N) depends on the particles' dimensions and on their orientations α (α is the angle of the particle in comparison with the theoretical fluid direction).

The tortuosity calculated for an isotropic medium is independent of the α angle (average 45° value), and depends only on the porosity value and d-D ratio. For 2-5 μm rectangular particles (2-5 shape factor), it varies from 1.19 to 1.35 in the 1.2 to 0.1 void ratio range. For the same particles, with a low e = 0.1 and α = 90°, the theoretical tortuosity value climbs up to 1.85 and 2.15 for 50% and 100% anisotropy. The deviation of tortuosity values which is a function of the α angle clearly appears with the increasing anisotropy %: i.e. deviation zero in an isotropic medium and 1.28 to 1.85 in a total anisotropic medium (calculated with e = 0.50). The 2-5 rectangular particle arrangement from a primary isotropic matrix to an oriented one generates a first anisotropy of tortuosity which is limited to a factor 2. The lengthening and stretching of the particles generates a higher and drastic tortuosity anisotropy which can reach a factor 10 or more (Fig.1(b)). That is the typical type of deformation that can affect the clay particles in the shear band.

2) Image analysis approach

Random images, i.e. uniform and isotropic 2D spatial distributions of rectangular particles, were made according to a derived Poisson's model. This model, which is closed to a hard-core process, avoids the interpenetration of particles /21/. This last hypothesis is based on the edge-to-edge or face—to-face vision of particle arrangement as a function of the applied pressure. The particle size distribution was chosen according to the granular curve, spread over nearly three decades (0.1 to 100 μm). A log-normal distribution was chosen to model the size distribution of particles. The main axes of particles are uniformly oriented in a defined angular sector (360° for an isotropic media, <360° for an anisotropic one. Following this simulation and according to its restricted hypotheses, we saw that the lower limit of porosity, with regard to the isotropic particle arrangement, is about 32 % (e=0.47). The only way to decrease the porosity according to the model is to admit anisotropy.

In this early and simple model, the tortuosity parameter is taken as the shortest path connecting the top

and bottom edges of the image and was determined by Monte-Carlo simulations /19/. If the compaction process is followed and an isotropic state is conserved, the tortuosity does not increase significantly and seems to be close to 1.13.

Consequences on hydraulic conductivity calculations

In the k versus e diagram, the clay specific surface increasing causes a vertical translation of the k curves (Fig.2(b)). In order to compare the different k evolutions as a function of e, particle orientation α, and the anisotropy %, the same specific surface (52.11 m^2/g) was used in the following calculations. The k curves are parallel for constant T values. Calculated with T as a variable function of e, the k curves show a slight difference in slope for the low e value domain. The simple orientation of particles and the associated T increase shift down the k curve by a maximum factor 2. The stretching of particles from 2-5 to 1-10 shifts down the k values drastically by a factor 10 (Fig. 2(b)).

Limits of theoretical hydraulic conductivity curves

The high initial porosity of a matrix formed by flocculation processes (75 – 90%) decreases to a lower value which is only governed by the d-D shape factor of the particles and by particle size distribution (median size, standard deviation, log or normal log repartition). Our calculations for 2-5 rectangular particles and normal log size repartition give a lower porosity limit of about 32% in an isotropic medium. The consequences of compaction and shearing processes are (1) to condense the material down to this lowest porosity value with respect to the isotropic edge –to-edge CVL microstructure, (2) to orientate the particles progressively, and (3) to dislodge and to stretch the particles so that they are face-to-face oriented.

The microstructure of the particle assemblage limits the hydraulic conductivity curves in the low porosity domain (Fig.2 (b)). The upper k curve, characteristic of the isotropic microstructure ($K_{isotrope\ (2/5)}$), is unrealistic for void ratio < 0.47. The void ratio limits of the k curves characteristic of partly oriented matrix progressively decrease to lower values when they shift down to the $K_{anisotrope\ (2/5)}$ curve. The void ratio limit of the 100% anisotropic matrix with stretched particles ($K_{stretched\ p.\ (1/10)}$) approaches zero. Finally, the decrease of the lower void ratio limit as a function of the anisotropy % defines an unrealistic domain of the material state (dashed area, Fig.2 (b)). From the inferior porosity limit of the isotropic domain two trends may exist: trend (1), which is governed by the simple arrangement of the particles, and trend (2), governed by the arrangement + local stretching of the particles. The more general trend (3) includes the compaction stage down to the isotropic microstructure $K_{isotrope\ (2/5)}$ curve, the superimposition of the compaction + arrangement stage down to the 100% anisotropic microstructure $K_{anisotrope\ (2/5)}$ curve and superimposition of the compaction + arrangement + stretching of particles down to the $K_{stretched\ P.(1/10)}$ curve. Trend (3) is characterised by slopes of the k curves higher than slopes of the calculated k curves. This is typical of experimental k curves whatever the sediment mineralogy: kaolinite, illite or smectite /22/.

CAM-CLAY diagram and hydraulic conductivity curve relations

The e versus log p CAM-CLAY diagram is crosscut by three parallel lines: VCL projection, CSL projection and "shear plane line". The simple consolidation stage shifts the material state from the e-axis to the VCL projection respecting the initial isotropic characteristic of the material (I_{600}; Fig. 1 (a)). The over-consolidation stage shifts the material state towards the CSL projection (I_{600} to I_{300}, I_{200}, I_{100}) respecting also the isotropic nature of the material. In these conditions the VCL-CSL band is divided into two parts : the upper part (1), above the I_{600}-I_{100} over-consolidation line, in which the material remains isotropic, and the lower part (2), under the I_{600}-I_{100} line, where the material is reorganised and more and more anisotropic (I_{100}-A_{100} to I_{600}-A_{600} trend). In the k versus e diagram, the two domains 1 and 2 are based on the $K_{isotrope\ (2/5)}$ and $K_{anisotrope\ (2/5)}$ curves respectively (Fig.2a). The state trend $I_{600} - A_{600} - S_{600}$ described in the e log p diagram associates e and anisotropy % which increase simultaneously. The calculation of k for these e values and associated tortuosities demonstrates the hydraulic conductivity trend $I_{600} - A_{600} - S_{600}$ of the same material in the k versus e diagram (Fig.2b).

In these VCL-CSL and $K_{isotrope\ (2/5)}$- $K_{anisotrope\ (2/5)}$ associated domains the increasing of Δe corresponds to a volume of expelled water. The micro-rearrangement of the particle is associated to the *in situ* and micrometric hydraulic conductivity changes which locally govern the water expulsion mechanisms.

The shift from the initial material state to the "Shear plane line" corresponds to a void ratio decrease plus change of the shape factor of the particle (S_{600}; Fig. 2(a)). The particle stretching modifies the hydraulic conductivity through the simultaneous e decreasing and tortuosity increasing (domain 3, Fig. 2(b)). The arrangement and stretching of particles creates a drastic anisotropy of the hydraulic conductivity in the shear bands.

CONCLUSION

This work focuses on the relations which can exist between the arrangement of the particles and the intrinsic hydraulic conductivity in order to explain how clay is mechanically damaged. The hydraulic conductivity curves calculated for the different microtextures delimit parallel domains, in the k versus e diagram, which can be associated with the "microtextural domains" of the CAM-CLAY representation. The anisotropy % of the particle arrangement induces an anisotropy of hydraulic conductivity which characterises each microtextural state of the material. This hydraulic conductivity anisotropy has a dominant role in the mechanisms of water flow and expulsion at the micrometric scale and consequently on the rotation of the particles. The particles stretching causes a drastic anisotropy of the hydraulic conductivity in the shear plane environment which has a dominant role in the post peak sliding. Tested on kaolinitic matrices mechanically damaged in the laboratory, the method shows: (1) the importance of the microstructural characterisation of a

clay matrix for a better understanding of its mechanical and hydraulic properties and (2) the importance of numeric petrography as a tool to establish the micro-meso relationships when clayey material is damaged.

REFERENCES

1. A.W. Skempton, The consolidation of clays by gravitational compaction. *Q. Jl. Geol. Soc. Lond.* **125**, (99), 373-411 (1970).
2. H. Rieke and G.V. Chilingarian, Compaction of argillaceous sediments, in: *Developments in Sedimentology,* 16, Elsevier Scientific Publishing Company, Amsterdam, 1974; p. 424..
3. J. Arch and A. Maltman, Anisotropic permeability and tortuosity wet sediments. *Jour. Geophys .Res.*, **95** (B6), 9035-9045 (1990).
4. F.J. Griffiths, and R.C. Joschi, Clay fabric response to consolidation. *Applied Clay Science,* **5**, 37-66 (1990).
5. J.A. Little, D. Muir-Wood, M.A. Paul, and A. Bouazza, Some laboratory measurements of permeability of Bothkennar clay in relation to soil fabric. *Géotechnique,* **42**, 335-361 (1992).
6. X. Luo, F. Brigaud, and G. Vasseur, Compaction coefficient of argillaceous sediments: their implications, significance and determination, *Norw. Petro. Soc.*, 321-332, 1993.
7. R.H. Bennett, W.R. Bryant, and M.H. Hubert, Microstructure of the fine clay sediments, in: *From Mud to Shale*, Springer-Verlag, New York.1994; pp. 567.
8. N.R. Morgenstern, and J.S. Tchalenko, The optical determination of preferred orientation in clays and its applications to the study of microstructure in consolidated kaolin. *Proc. Royal Soc.* **A300**, 218-250 (1967).
9. J.E. Gillot, Study of the fabric of fine-grained sediments with the scanning electron microscope. *J. Sediment. Petrol.* **39**, 90-105 (1969).
10. R.H. Foster and P.K. De, Optical and electron microscopic investigation of shear induced structures in lightly consolidated (soft) and heavily consolidated (hard) kaolinite. *Clay and Clay Min.* **19**, 31-47 (1971).
11. E. Mc Kyes and R.N. Yong, Results of three technics for fabric viewing as applied to shear distortion of clay. *Clays and Clay Min.* **19**, 5 (1971).
12. X. Bai and P. Smart, Change in microstructure of kaolin in consolidation and undrained shear. *Géotechnique,* **47** (5), 1009-1017 (1997).
13. P. Dudoignon and A. Pantet, Measurement and cartography of clay matrix orientations by image analysis and grey-level diagram decomposition, *Clay Minerals*, **33**, 629-642 (1998).
14. P. Dudoignon, A. Pantet, L. Carrara and B. Velde, Macro-micro measurement of particle arrangement in sheared kaolinitic matrices, *Géotechnique*, **51** (6), 493-499 (2001).
15. J. Pantaloni, Ecoulement de fluide. Ecoulement en milieu poreux, Séminaire "Les procédés de

separation", 6-7 8 spt. Paris, Comite français de l'électricité, 32p, 1988.

16. J. Grollier, J. Fernandez, M. Hucher, and J. Riss, *Les proprietés physiques des roches, Théories et modèles*. Masson edn. 462 p., 1991.
17. Y.W. Tsang, The effect of tortuosity on fluid flow through a single fracture, *Water Resour. Res.*, **20** (9), 1209-1215 (1984).
18. J. Dvorkin, H. Gvirtzman, and A. Nur, Kozeny-Carman relation for a medium with tapered cracks, *Geophys. Res. Lett.*, **18** (5), 877-880 (1991).
19. S. Sammartino, P. Sardini, E. Moreau, and G. Touchard, Connectivity evolution of 2D random distributions of disks and ellipses: Application to polyphasic crystal rock distribution, *Acta Stereologica*, **17** (3), 309-314 (1998).
20. P. Sardini, S. Sammartino, E. Moreau, A. Meunier, and E. Tevissen, Evolution of Fluid Pathways of Charroux-Civray Tonalite (part II): Numerical Study of Microcrack Networks, *Physics and Chemistry of the Earth (A)*, **24** (7), 621-625 (1999).
21. M. Coster and J.-L. Chermant, *Précis d'analyse d'images*, Presses du C.N.R.S., 560 p., 1989.
22. I. Djéran-Maigre, D. Tessier, D. Grunberger, B. Velde and G. Vasseur, Evolution of microstructures and of macroscopic properties of some clays during experimental compaction. *Marine and Petroleum Geology*, **15**, 109-128 (1998).